Digitally Reconfigurable Transmitarray With Beam-Steering and Polarization Switching Capabilities

BISWARUP RANA[1], **IN-GON LEE**[1], **AND IC-PYO HONG**[2], **(Member, IEEE)**

[1]Smart Natural Space Research Centre, Kongju National University, Cheonan 31080, South Korea
[2]Department of Information and Communication Engineering, Kongju National University, Cheonan 31080, South Korea

Corresponding author: Ic-Pyo Hong (iphong@kongju.ac.kr)

ABSTRACT In this paper, a novel digitally reconfigurable unit-cell and 4 × 4 transmitarray operating at X-band is proposed that allows the implementation of beamforming and polarization conversion operations in a programmable way. The lower layer of transmitarray responsible for beam steering consists of two PIN diodes and a circular type patch which has two states of operations with 0 and π phase responses which we name ''State1'' and ''State2''. ''State1'' and ''State2'' can be represented by a digital notation as ''1'' and ''0'' elements. Similarly, the upper layer of the transmitarray responsible for polarization conversion operation consists of two states of operation which we name as ''State3'' and ''State4'', respectively. ''State3'' and ''State4'' also can be represented by digital notations as ''1'' or ''0'' elements. By coding ''0'' and ''1'' elements for the lower side of the transmitarray in a 1-bit sequence, we can steer the beam in our desired direction. Similarly, by coding ''0'' and ''1'' elements in a 1-bit sequence element for the upper layer, we can get X-polarized and Y-polarized beams. Combining the upper layer 1-bit sequence and lower layer 1-bit sequence, we can get both polarization conversion and beam steering simultaneously. A 4 × 4 array with our proposed unit cell was designed and fabricated. A good agreement between simulated and measured results was observed. The proposed design is a promising concept because it can be fabricated using the conventional fabrication process, it is cost-effective compared to conventional phased array antenna for satellite and radar applications. A 4 × 4 array was taken just to check the transmission and reflection coefficients of the proposed unit cells. A very small transmitarray was manufactured and experimentally characterized just as a proof of concept, to verify that the unit cells work properly.

INDEX TERMS Reconfigurable transmitarray, beam steering, polarization conversion, X-band, unit-cell.

I. INTRODUCTION

Recently with the advance of coding meta-surface and digital meta-surface, there is a great interest in developing digitally coded surfaces for beam steering and polarization conversion among the antenna community [1]–[10]. To steer the beam in different directions and get polarization converted waves, conventionally phases array antennas are being used [11]. However, traditional phased array antennas are expensive, bulky, and complex. The phase shifters used in the conventional phased array antennas have a high insertion loss. Generally, a power amplifier is used to enhance the signal

strength for conventional phased array antennas. Low insertion loss, lightweight, low profile, and low-cost antennas with beam steering and polarization conversion operation are required for radar and satellite communication applications. Conventional phased array antennas are being used for such applications, which are bulky, expensive, and analog. Transmitarray is one of the promising candidates that can replace conventional phased array antennas for beam scanning and polarization conversion operations [12]–[32]. The identical unit cells that are the building block of transmitarrays are arranged periodically. A source antenna like a horn or patch array is kept at a suitable distance in front of the transmitarray to manipulate the EM waves in the desired direction. Frequency selective surface, microstrip patches,

The associate editor coordinating the review of this manuscript and approving it for publication was Lu Guo .

or metamaterial structures are generally considered for the unit cells of the transmitarrays. Conventional printed circuit board (PCB) technology is used to fabricate the unit cells and the entire transmitarray. The first transmitarray was proposed by McGrath in 1984 connecting an upper patch and lower patch through a via-hole [12]. There are two types of transmitarray in the literature a) passive transmitarray b) active transmitarray for beam-steering operation. Passive transmitarray has no active component like varactor diode or PIN diode whereas active transmitarray has active components like PIN diode or varactor diode. In the literature, several passive transmitarrays were presented for beam steering operations [13]–[16]. In [13], the authors proposed a beam-steering antenna for ground mobile terminals of Ka-band satellite and high-altitude platform. In [14], a dual-band high gain passive transmitarray was proposed for Satcom terminals. A V-band switched-beam transmitarray was proposed for wireless backhaul applications in [15]. A 3D printed perforated transmitarray was proposed for beam scanning operation in [16]. In [17], first, an active transmitarray prototype was proposed and a 360° reflective-type phase shifter was used in that design to scan the beam. Since then, different authors have proposed different transmitarrays. There are two types of active transmitarray a) analog-type active transmitarray b) digital-type active transmitarray.

In the case of analog-type transmitarray, 360° phase shifters are used for beam steering operation. Generally, reflective type phase shifters with varactor diodes are used which have a phase shift range of 360° or more [17]. However, these reflective-type phase shifters are lossy and the total performance of the transmitarray degrades significantly with these reflective-type phase shifters. To overcome this problem, a novel design approach was presented in where the reflective-type phase shifter with power amplifier was used [18]. However, the proposed design suffered from undesired coupling effects because of complicated bias networks for controlling the active components to achieve multifunction, and the complexity can be increased depending upon the number of the unit-cell. In the literature, most of the authors have focused only on the beam steering of the transmitarray. There are very few works on both polarization conversion and beam steering operations. In [19], a transmitarray was proposed that had both beam steering and polarization conversion capabilities. However, a reflective type phase shifter was used with varactor diodes for the phase-shifting operation that made the design analog type. The transmitarray was composed of an active patch, a 360° reflective-type phase shifter, and a passive patch. Two cascaded quadrature bridge structures were used to make the 360° reflective-type phase shifter and each structure had a four-port directional coupler. Varactor diodes were used to realize the phase shifter. By varying the bias voltage, the capacitance of the varactor diode could be varied from 0.17 to 1.1 pF. Those varactor diodes make the transmitarray analog type. Two PIN diodes were used on the upper patch for the polarization conversion operation.

In the case of digital-type transmitarrays, the phase of the input signals is discretized with PIN diodes. 360° phase can be discretized into 1-bit (0°/180°) or 2-bit (0°/90°/180°/270°). Therefore, it is more efficient to implement a digitally reconfigurable transmitarray. In [20], the authors proposed an electronically reconfigurable unit cell to achieve beam steering operation. The structure had two rectangular patches loaded with U-and O-type slots. The passive patch had no PIN diode but the active patch had two PIN diodes and a single bias line for beam steering operation. The design showed wide impedance bandwidth and low insertion loss. The same unit cell was used to design an 20×20 array in [21]. However, the design had only beam scanning capability. In [22] authors had proposed a digitally control transmitarray. There were two-layer metallic patterns connected by a metallic via-hole. One layer of metallic layer had two PIN diodes and another layer of metallic layer had another two PIN diodes. The design was experimentally verified in an ad-hoc waveguide simulator.

Electronically polarization switching is now very important in modern communication devices. In [23], an electronically reconfigurable polarization converter was presented at X-band. A new method to measure the performance of the unit cells for the polarization conversion was also proposed in that paper using X-band WR-90 wave and rectangular to square waveguide transition section. The performance of the overall 2×2 unit-cells was verified with an X-band miniaturized horn antenna and satisfactory results were obtained.

In this paper, a novel type wideband 1-bit (0°/180°) digitally reconfigurable unit cell is proposed using PIN diodes for both polarization conversion and beam steering operations. To the authors' best knowledge such type of transmitarray with fabricated array has yet not been reported in the literature which has both beam steering and polarization conversion capabilities. We have used two PIN diodes for beam steering operation and another two PIN diodes for polarization conversion operation. So, beam steering operation and polarization conversion operations can be achieved by the digital form instead of the analog. The proposed array produces lower losses at our desired frequencies compare to ordinary microstrip phased array antennas or metallic phased array antennas. The paper is expected to give a significant advancement of the transmitarray as a new type of digitally coded transmitarray with different functionalities. The main objective of this research is to develop a new type of transmitarray for next-generation radar applications which are less expensive, low loss, consume less amount of power compared to convention phased array antennas. The digitally reconfigurable technique used in this design enables the transmitarray to be controlled digitally by a field-programmable gate array (FPGA) or any other microcontroller for beam steering and polarization conversion operations. We have conceived a term named ''Digital Electromagnetics'' where electromagnetic waves are supposed to digitize for various applications without using conventional phase shifters.

The remainder of this paper is arranged in the following way. In Section II, the configuration and performance of the unit cell are discussed while in Section III, the equivalent circuit model of the unit cell is presented. The design of the 4×4-unit cell array is described in Section IV and the electrical circuit model of the one row of the 4×4 array is described in Section V. In Section VI, a measurement technique to measure the polarization conversion operation is presented. Lastly, a conclusion is made for the proposed unit cell and 4×4 array.

II. CONFIGURATION AND PERFORMANCE OF THE UNIT CELL

Ansys Electronics Desktop simulator was used to simulate the proposed unit cell as well as 4×4-unit cells with horn antennas. A normal plane wave impinging upon a unit cell with master-slave boundary conditions was used to simulate the unit cell. The element was designed at the center frequency of 9.5 GHz. 3D view of the proposed unit cell is shown in Figure 1.

Two Taconic substrates with permittivity of 3.5, loss tangent of 0.0018, and height of 1.52 mm each bonded by a bonding film with permittivity of 3.88, loss tangent of 0.0236 was considered for our design. The area of the unit cell was 15×15 mm^2. A metalized via-hole with a diameter of 0.4 mm at the middle of the unit cell connects upper and lower patches. A bias line in between lower Taconic substrate and bonding film with a metalized via hole with a diameter of 0.4 mm was introduced to give dc power supply to lower two PIN diodes. To give dc power to the upper two PIN diodes, another bias line was designed on the top Taconic substrate as shown in Figure 1. The size of the unit cell is $0.47\lambda_0 \times 0.47\lambda_0$. Figure 2(a) and (b) show the top view of the patch for polarization conversion and the bottom view
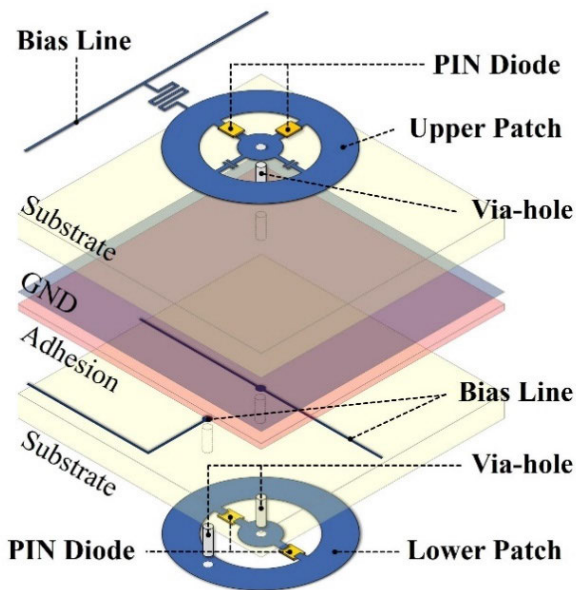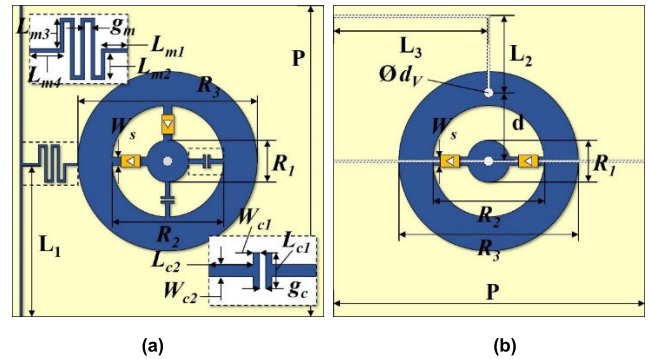

FIGURE 1. 3D view of the unit cell.

FIGURE 2. (a) Top view of the unit cell (b) Bottom view of the unit cell.

for beam steering of the proposed unit cell, respectively. The upper patch has two PIN diodes (MA4GP907, MACON, Lowel, MA, USA) for polarization conversion operation and the lower patch has also two same PIN diodes for beam steering operation. To minimize the biasing line effect on the top patches, a resonator ($L_{m1} = 0.1$ mm, $L_{m2} = 0.8$ mm, $L_{m3} = 0.9$ mm, $L_{m4} = 0.9$ mm and $g_m = 0.2$ mm) was also conceived as shown in Figure 2(a). To compensate, the capacitance introduced by PIN diodes on the upper patches, an equivalent capacitance ($L_{C1} = 0.6$ mm, $L_{C2} = 0.7$ mm, $W_{c2} = 0.2$ mm, and $g_c = 0.1$ mm) was conceived. Both upper and lower patch has a circular type of slots to enhance the operational bandwidth of the unit cell. The other parameters of Figure 1 are $L_1 = 7.2$ mm, $W_S = 0.38$ mm, $R_3 = 8.4$ mm, $R_1 = 1.0$ mm, $R_2 = 4.8$ mm, $P = 15$ mm, $d = 3.2$ mm, $L_2 = 4$ mm and $L_3 = 7.3$ mm. The equivalent circuit model of the PIN diode for both forward and reverse bias conditions are shown in Figure 3($L_{11} = 0.05$ nH, $R_{11} = 2.1 \ \Omega$ for the forward bias condition and $L_{22} = 0.05$ nH, $R_{22} = 300$ KΩ, $C_{22} = 50$ fF for the reverse bias condition). In this paper, "State1" represents when both polarization conversion and phase-shifting operations of the unit cell are in an "Off State". "State2" represents when the polarization conversion is "Off State" and phase-shifting operation is "On State". "State3" represents when the phase-shifting operation is "Off State" and polarization conversion is "On State". Lastly, "State4" represents when the phase-shifting operation is "On State" and polarization conversion is also "On State". Table 1 lists the main feature of the unit cell.

Figure 4(a) shows the magnitude of transmission and reflection coefficients for "State1" and "State2" of the proposed unit cell. -3 dB transmission bandwidths for "State1" and "State2" are 540 MHz (9.14-9.68 GHz) and 450 MHz (9.22-9.67 GHz), respectively. Figure 4(b) depicts the magnitude of transmission and reflection coefficients for "State3" and "State4" of the unit cell and -3 dB transmission bandwidth for "State3" and "State4" are 490 MHz (9.22-9.71 GHz) and 560 MHz (9.17-9.73 GHz), respectively. The phase of the incoming signals is changed at the lower patch of the unit cell and it is depicted in Figure 5. It is observed that the phase is -12° at 9.5 GHz for "State1" and 172° at the same frequency for "State2".
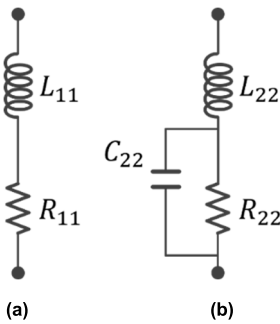
FIGURE 3. Equivalent circuit of the PIN diode (a) On condition (b) Off condition.

TABLE 1. Main features of the unit cell.

No.	PARAMETERS	Values
1	Unit-cell size	15 mm ($0.47\lambda_0$) $\times$ 15 mm ($0.47\lambda_0$)
2	Patch diameter	8.4 mm
3	Slot diameter	4.8 mm
4	Substrate	Taconic RF 35 (ε_r=3.5, tanδ= 0.0018, h=1.52 mm)
5	Boding film	ε_r=3.88, tanδ= 0.0236, h=0.1 mm
6	Dimeter of connecting via	0.4 mm
7	Dimeter of bias via	0.4 mm
8	Ground plane opening diameter	0.7 mm
10	PIN diode	MA4GP907; MACOM, Lowell, MA, USA

A phase shift of 184° was observed while biasing conditions of the PIN diodes of the lower patch were changed. The surface current distributions of the lower and upper patch of the unit cell for different biasing conditions are depicted in Figure 6. Figure 6 (a) and Figure 6 (b) show the top and bottom surface current distributions for State1 while Figure 6 (c) and Figure 6 (d) show the bottom and top surface current distributions for State2. Figure 6 (e) and Figure 6 (f) show bottom surface current distributions for State 3 and State 4.

III. EQUIVALENT CIRCUIT MODELLING OF UNIT-CELL

The equivalent circuit model of the proposed unit cell is shown in Figure 7. The upper and lower slots loaded circular patches that can be modeled as equivalent impedance. The upper patch was modeled as Z_1 and Z_2 impedances while the lower patch was modeled as Z_6 and Z_8 impedances. The upper and lower patch both are in the air and that can be modeled as an ideal transformer with 377 Ω port impedances. The top and bottom patches both have two PIN diodes each. The PIN diodes can be modeled as impedances Z_4 and Z_3 for forward and reverse conditions. Due to the bulk volume of the diodes, a series capacitance C_2 and shunt capacitance C_1 were conceived to compensate capacitance introduced by the upper PIN didoes. Similarly, the lower patch has two PIN diodes that can be modeled as equivalent impedance Z_5 and Z_7 respectively for forward and reverse bias conditions. The PIN
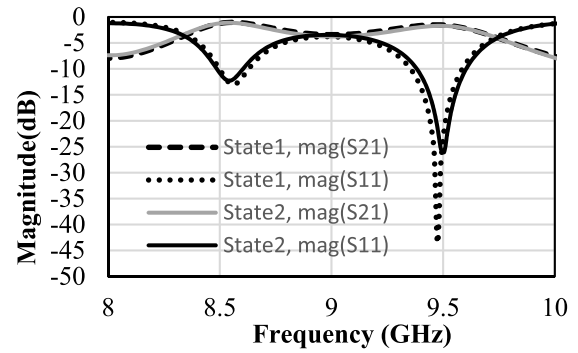
(a)
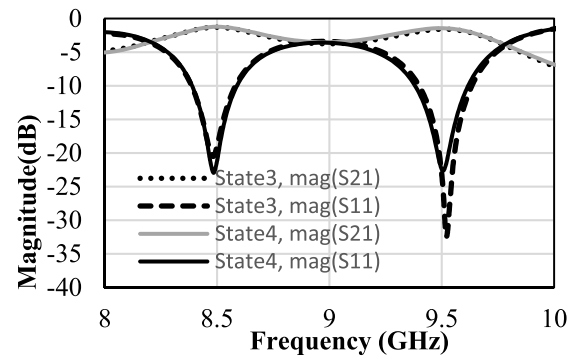
(b)

FIGURE 4. Magnitude of transmission and reflections coefficients of the unit cell for (a) State1 and State2 (b) State3 and State4.
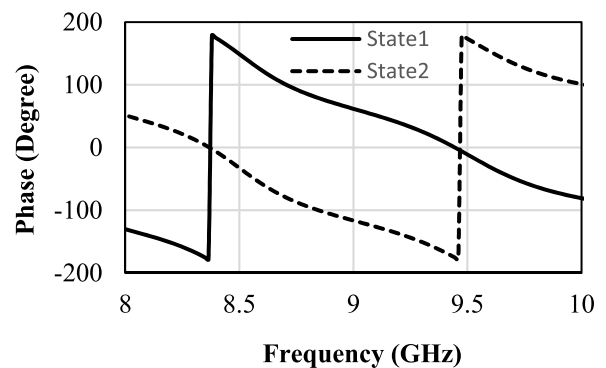

FIGURE 5. Phase of the transmission coefficients of the unit cell.

diodes on the bottom patch introduced an equivalent capacitance that can be compensated with a series capacitance C_4 and shunt capacitance C_5. Our circuit model is similar to the circuit model published in [20].

IV. DESIGN OF THE 4 × 4 ARRAY

Figure 8 shows a schematic view of the 4 × 4 array with detailed dimensions as L_{21} = 117.9 mm, L_{22} = 60 mm, L_{23} = 34 mm, L_{24} = 15 mm, W_{21} = 90 mm, W_{22} = 60 mm, and W_{23} = 46.1 mm. To validate our proposed concept, a 4 × 4 array was conceived and designed. The same Taconic substrate with the same parameters as the unit cell was considered while designing the array. Figure 9 shows
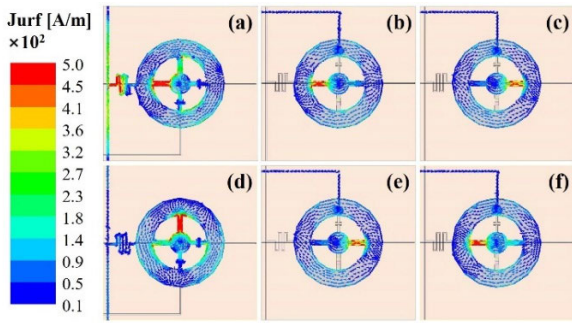
FIGURE 6. Surface current distributions of the unit cell for different biasing conditions (a) Top view for State1 (b) Bottom view for State1 (c) Bottom view for State2 (d) Top view for State2 (e) Bottom view for State3 (f) Bottom view for State4.
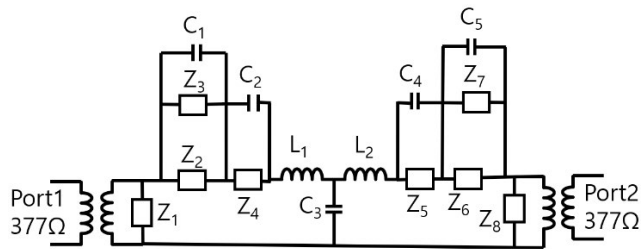

FIGURE 7. Equivalent circuit of the unit cell.

the top view of the 4×4 array and its biasing line for the polarization conversion operation. As our desired polarization was two orthogonal polarizations namely X-polarization and Y-polarization, all bias lines were connected. And lastly, one signal bias line with a width of 0.1 mm was connected to the D-sub connector.

The ground plane has only one opening for the central via-hole with a diameter of 0.7 mm that connects upper and lower patches. There is a bonding layer with a permittivity of 3.88, loss tangent of 0.0236 below the ground plane and above the lower substrate. The bias line configuration for beam steering operation is depicted in Figure 10. The width of the bias line is 0.1 mm and the separation between the bias lines for a single row of the bias line is 0.1 mm. With that
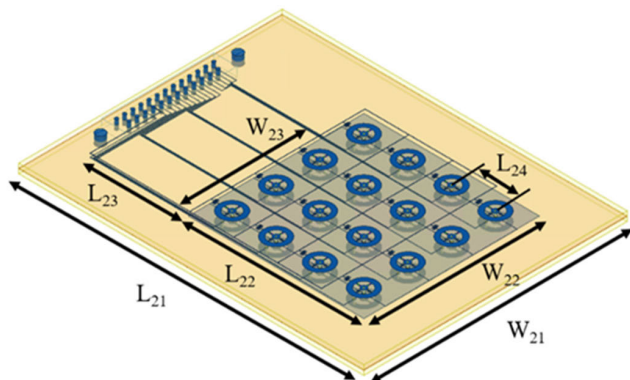

FIGURE 8. Schematic view of the 4×4 array design with details dimensions.
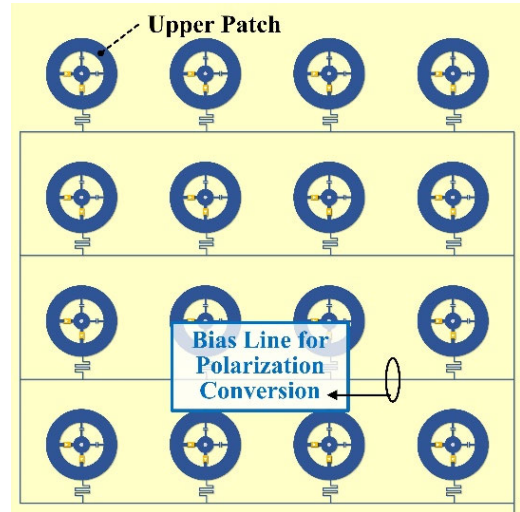

FIGURE 9. Top view of the 4×4 array.

width of the bias lines and spacing between the bias lines, there was very less effect of the bias lines with the overall performance of the 4×4 array.

V. ELECTRICAL CIRCUIT DIAGRAM OF THE PROPOSED ARRAY

The electrical circuit diagram of the one row of the proposed 4×4 array is depicted in Figure 11. The upper side of the circuit diagram with two PIN diodes is similar to that of the lower side of the circuit diagram. Two PIN didoes were connected back-to-back for both the upper patch and lower patch. A metalized via-hole connected the upper patch and lower patches. There is a connection between the unit cells by a common line that acts as a ground plane. A voltage source of 3.3 V was used for the 4×4 array. The maximum power dissipation of our proposed 4×4 array is 640 mW provided minimum voltage is applied. The biasing lines were
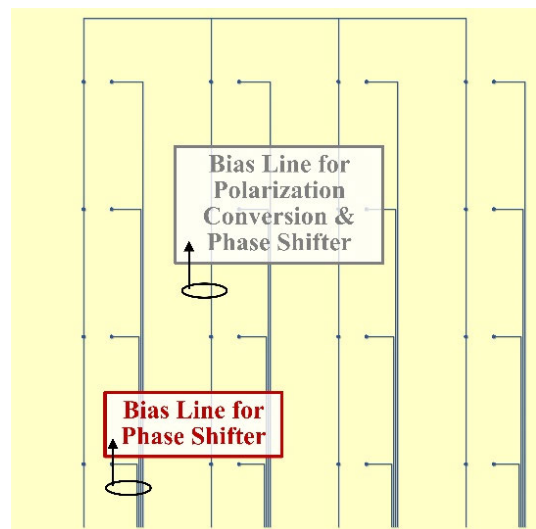

FIGURE 10. Bias line view of the 4×4 array.

kept inside to minimize the effect of biasing lines on the unit cell performance. It was found through simulation that the biasing line had no significant effect on the performance of the unit cell and 4 × 4 array.
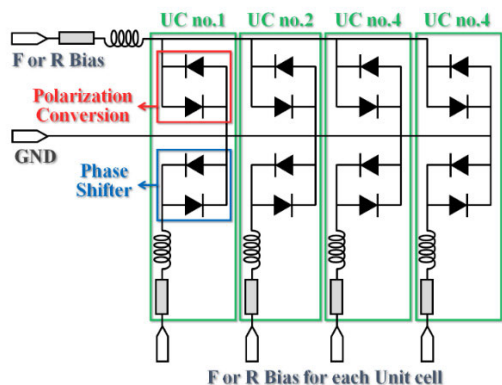

FIGURE 11. Circuit diagram of one row of the unit cells (1 × 4).

VI. EXPERIMENTAL METHOD

To measure the polarization conversion operation and verify transmission characteristics of the proposed 4 × 4 transmitarray, a free space measurement method illustrated in Figure 12 was used. The measurement setup consisted of a transmitting antenna (WR-90, gain: 10 dB, frequency: 8.2–12.4 GHz) and the same type of receiving antenna.

Outside of the transmitarray, pyramidical absorbers were kept to minimize the interference caused by diffraction by the edge of the transmitarray, the Zig, the edge, and the measuring equipment. The magnitude and phase of the transmitted and reflected signals can be measured according to the permittivity and geometry of the transmitarray. The distance between the aperture of the standard X-band horn antennas was 318 mm and transmitarray was placed 15 mm from the transmission in between the horn antennas. The distance between the receiving aperture of the horn antenna and the transmitarray was kept in such a way so that the transmitarray under test was more than the far-field distance of the operating frequency. The design frequency of the transmitarray was 9.5 GHz. As the dimension of the aperture is very small, placing the aperture far from the horn antenna can give a spillover effect. Thus, we have placed the transmitarray in such distance so that we can get transmission and reflection coefficient properly. The horn antenna does not have a plane wavefront. However, as we are discretizing 360° phase range into 1-bit (0°/180°), some unit cell has certain phase and some other unit cell has some different phase. But the other unit cell has no large phase shift compared to central unit cells making them useful for 1-bit operation. This phase mismatch between the unit cells causes some gain degradation of the transmitarray. Figure 13 shows the top view and bottom view of the fabricated transmitarray. Figure 14 shows the practical measurement setup for the proposed transmitarray. Figure 15, Figure 16, Figure 17, and Figure 18 show simulated and
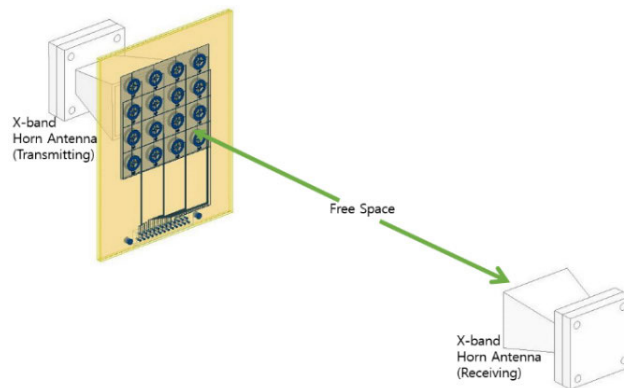

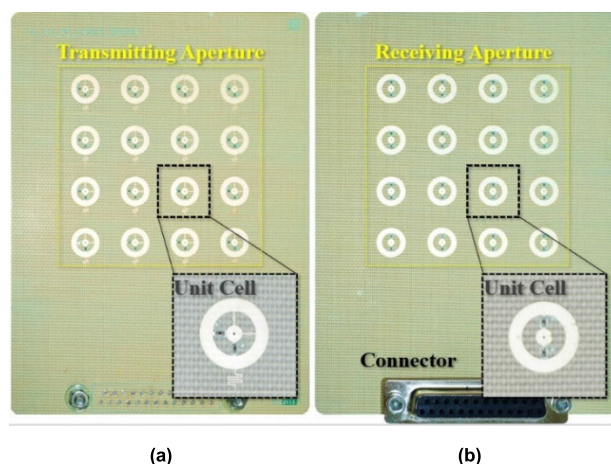**FIGURE 12.** Measurement setup for the proposed transmitarray.

(a)   (b)

FIGURE 13. (a) Photography of the fabricated transmitarray prototype consisting of 4 × 4-unit cells (a) Top view and (b) Bottom view.
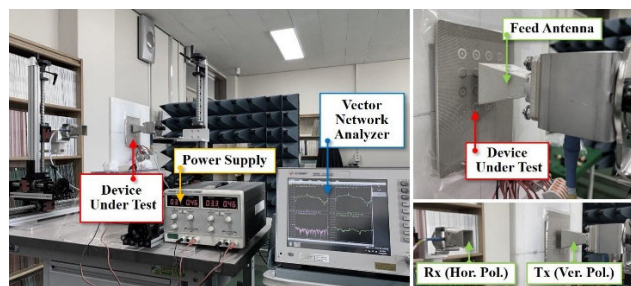

FIGURE 14. Practical measurement setup of the proposed transmitarray.

measured magnitude of transmission and reflection coefficients for State1, State 2, State 3, and State 4, respectively. The polarization conversion operation can be verified from Figure 17 and Figure 18. Figure 19 and Figure 20 show the simulated and measured phase of the transmission coefficients for State 1, State 2, State 3, and State 4. There was some discrepancy between the simulated and measured phase of the transmission coefficients. However, this discrepancy does not affect the overall performance of the transmitarray. Figure 21 shows the normalized radiation patterns at 9.5 GHz for polarization converted state and no polarization converted
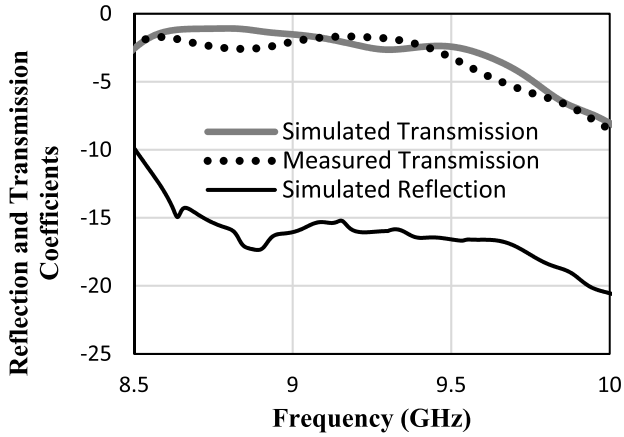
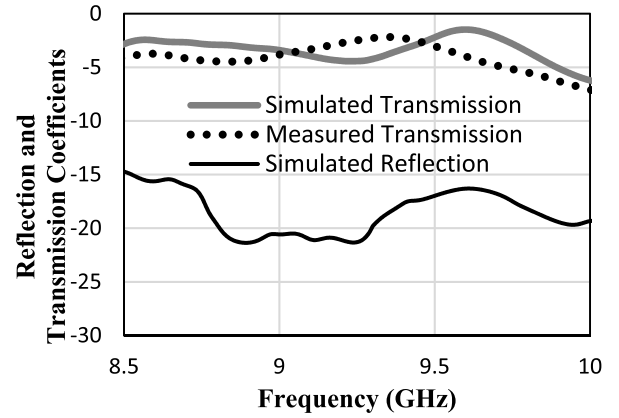**FIGURE 15.** Simulated and measured transmission and reflections coefficients for State1 of the 4 × 4 array.

FIGURE 16. Simulated and measured transmission and reflections coefficients for State2 of the 4 × 4 array.

FIGURE 17. Simulated and measured transmission and reflections coefficients for State3 of the 4 × 4 array.

FIGURE 18. Simulated and measured transmission and reflections coefficients for State4 of the 4 × 4 array.
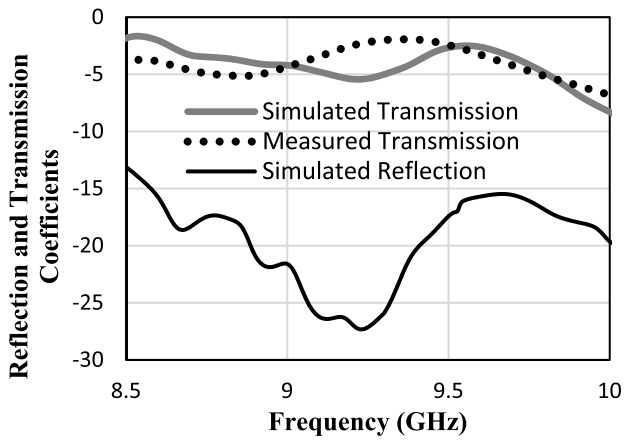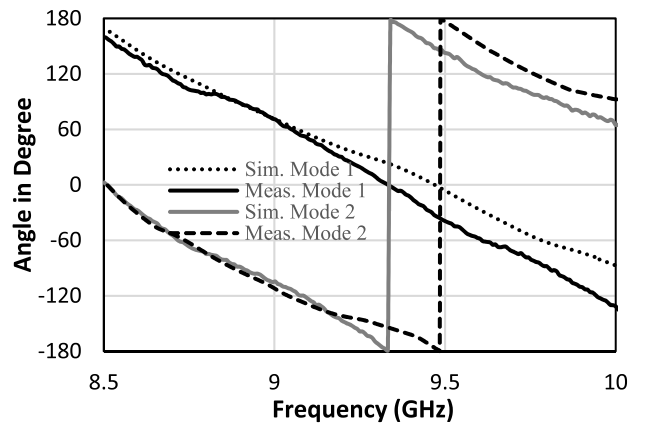

FIGURE 19. Simulated and measured phase of the transmission coefficients for State1 and State2 of the 4 × 4 array.
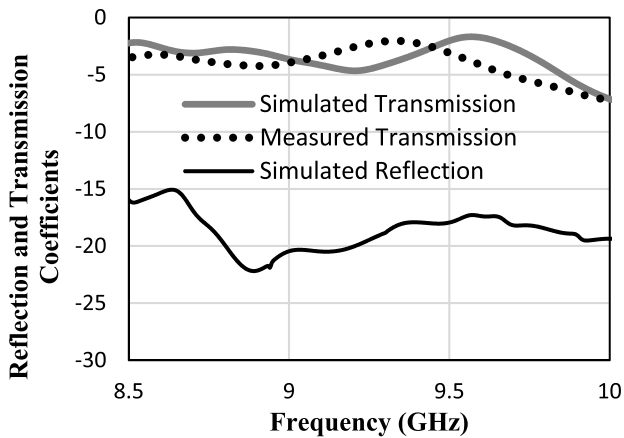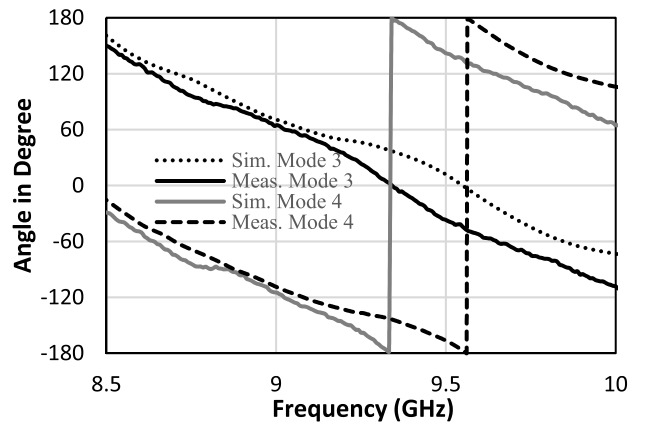

FIGURE 20. Simulated and measured phase of the transmission. coefficients for State3 and State4 of the 4 × 4 array.

state for $\varphi = 0°$ plane while Figure 22 shows normalized radiation patterns at 9.5 GHz for polarization converted state and no polarization converted state for $\varphi = 0°$ plane. The peak gain was at $\theta = 0°$ for Figure 21 and the peak gain was at $\theta = 15°$ for Figure 22.   A beam steering of 15° is observed

with our proposed 4 × 4 unit-cell for both polarizations converted state and no polarization converted state. So, both beam steering and polarization conversion operations can be verified from these radiation patterns. In [33], the authors used a near-field phase correction structure. In [34], a low profile phase correcting surface was introduced to improve
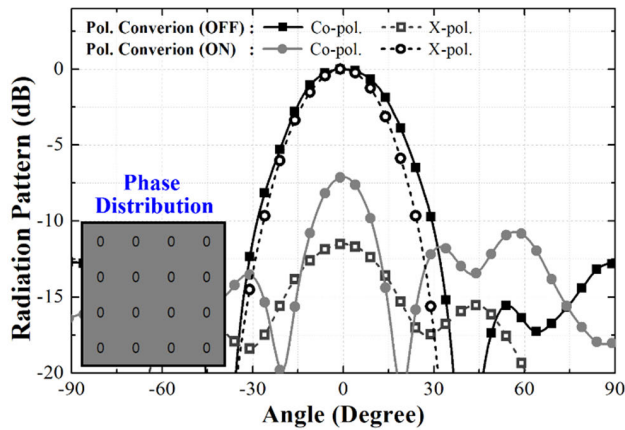
FIGURE 21. Simulated radiation patterns for polarization converted and no polarization converted state for $\varphi = 0°$ plane (peak gain at $\theta = 0°$).

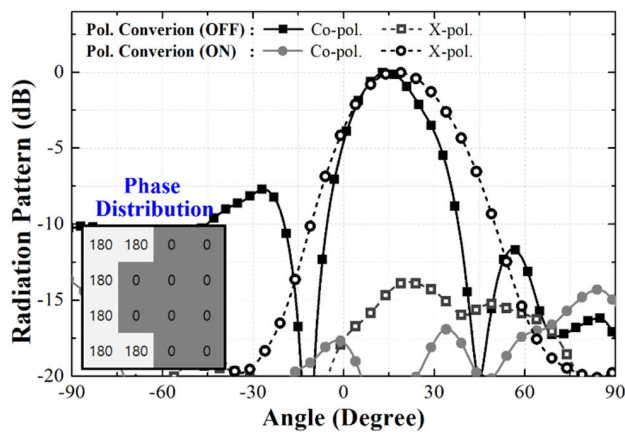**FIGURE 22.** Simulated radiation patterns for no polarization converted state for $\varphi = 0°$ plane (peak gain at $\theta = 15°$).

directive radiation. By using such structures, the efficiency of the measurement setup would have been increased for our structure. However, in our measurement setup, we have not used such structures. While measuring the transmission and reflection coefficients, the states of the all-unit cell were the same state. However, the unit cells were different states for 15° beam steering. Using a 4 × 4 array, a 15° scanning angle can be achieved. However, with an 8 × 8 or 16 × 16 array, a larger scanning angle with better angular resolution can be achieved.

VII. CONCLUSION

In this paper, a digitally reconfigurable transmitarray has been proposed for beam steering and polarization conversion operations at X-band. A 4×4 array was conceived, fabricated, and tested. There is a total of four PIN diodes on each unit cell among them two for polarization conversion and two for beam steering operations. By changing the bias voltages of the four PIN diodes, the digital reconfigurable transmitarray gives four States. Both polarization conversion and beam steering operations were verified with the 4×4 array. A bigger

array with 8 × 8-unit cells or 16 × 16-unit cells can be fabricated for real-time applications.

REFERENCES

[1] L. Shao, M. Premaratne, and W. Zhu, "Dual-functional coding metasurfaces made of anisotropic all-dielectric resonators," *IEEE Access*, vol. 7, pp. 45716–45722, 2019.

[2] L. Zhang, Z. X. Wang, R. W. Shao, J. L. Shen, X. Q. Chen, X. Wan, Q. Cheng, and T. J. Cui, "Dynamically realizing arbitrary multi-bit programmable phases using a 2-bit time-domain coding metasurface," *IEEE Trans. Antennas Propag.*, vol. 68, no. 4, pp. 2984–2992, Apr. 2020.

[3] H. Taghvaee, A. Cabellos-Aparicio, J. Georgiou, and S. Abadal, "Error analysis of programmable metasurfaces for beam steering," *IEEE J. Emerg. Sel. Topics Circuits Syst.*, vol. 10, no. 1, pp. 62–74, Mar. 2020.

[4] D. Wang, L.-Z. Yin, T.-J. Huang, F.-Y. Han, Z.-W. Zhang, Y.-H. Tan, and P.-K. Liu, "Design of a 1 bit broadband space-time-coding digital metasurface element," *IEEE Antennas Wireless Propag. Lett.*, vol. 19, no. 4, pp. 611–615, Apr. 2020.

[5] H. Rajabalipanah, A. Abdolali, and K. Rouhi, "Reprogrammable spatiotemporally modulated graphene-based functional metasurfaces," *IEEE J. Emerg. Sel. Topics Circuits Syst.*, vol. 10, no. 1, pp. 75–87, Mar. 2020.

[6] T. J. Cui, M. Q. Qi, X. Wan, J. Zhao, and Q. Cheng, "Coding metamaterials, digital metamaterials and programmable metamaterials," *Light, Sci. Appl.*, vol. 3, no. 10, p. e218, Oct. 2014.

[7] S. Liu and T. J. Cui, "Concepts, working principles, and applications of coding and programmable metamaterials," *Adv. Opt. Mater.*, vol. 5, no. 22, Nov. 2017, Art. no. 1700624.

[8] T. J. Cui, S. Liu, and L. Zhang, "Information metamaterials and metasurfaces," *J. Mater. Chem. C*, vol. 5, no. 15, pp. 3644–3668, 2017.

[9] T. J. Cui, "Microwave metamaterials," *Nat. Sci. Rev.*, vol. 5, no. 2, pp. 134–136, 2018.

[10] T. J. Cui, "Microwave metamaterials—From passive to digital and programmable controls of electromagnetic waves," *J. Opt.*, vol. 19, no. 8, Aug. 2017, Art. no. 084004.

[11] S.-M. Moon, S. Yun, I.-B. Yom, and H. L. Lee, "Phased array shaped-beam satellite antenna with boosted-beam control," *IEEE Trans. Antennas Propag.*, vol. 67, no. 12, pp. 7633–7636, Dec. 2019.

[12] D. T. McGrath, "Planar three-dimensional constrained lenses," *IEEE Trans. Antennas Propag.*, vol. AP-34, no. 1, pp. 46–50, Jan. 1986.

[13] E. B. Lima, S. A. Matos, J. R. Costa, C. A. Fernandes, and N. J. G. Fonseca, "Circular polarization wide-angle beam steering at Ka-band by in-plane translation of a plate lens antenna," *IEEE Trans. Antennas Propag.*, vol. 63, no. 12, pp. 5443–5455, Dec. 2015.

[14] S. A. Matos, E. B. Lima, J. S. Silva, J. R. Costa, C. A. Fernandes, and N. J. G. Fonseca, "High gain dual-band beam-steering transmit array for satcom terminals at Ka-band," *IEEE Trans. Antennas Propag.*, vol. 65, no. 7, pp. 3528–3539, Jul. 2017.

[15] L. Dussopt, A. Moknache, J. Säily, A. Lamminen, M. Kaunisto, J. Aurinsalo, T. Bateman, and J. Francey, "A V-band switched-beam linearly polarized transmit-array antenna for wireless backhaul applications," *IEEE Trans. Antennas Propag.*, vol. 65, no. 12, pp. 6788–6793, Dec. 2017.

[16] A. Massaccesi, G. Dassano, and P. Pirinoli, "Beam scanning capabilities of a 3D-printed perforated dielectric transmitarray," *Electronics*, vol. 8, no. 4, p. 379, Mar. 2019.

[17] P. Padilla, A. Muñoz-Acevedo, M. Sierra-Castaner, and M. Sierra-Perez, "Electronically reconfigurable transmitarray at Ku band for microwave applications," *IEEE Trans. Antennas Propag.*, vol. 58, no. 8, pp. 2571–2579, Aug. 2010.

[18] W. Pan, C. Huang, X. Ma, and X. Luo, "An amplifying tunable transmitarray element," *IEEE Antennas Wireless Propag. Lett.*, vol. 13, pp. 702–705, 2014.

[19] C. Huang, W. Pan, X. Ma, B. Zhao, J. Cui, and X. Luo, "Using reconfigurable transmitarray to achieve beam-steering and polarization manipulation applications," *IEEE Trans. Antennas Propag.*, vol. 63, no. 11, pp. 4801–4810, Nov. 2015.

[20] A. Clemente, L. Dussopt, R. Sauleau, P. Potier, and P. Pouliguen, "1-bit reconfigurable unit cell based on PIN diodes for transmit-array applications in X band," *IEEE Trans. Antennas Propag.*, vol. 60, no. 5, pp. 2260–2269, May 2012.

[21] A. Clemente, L. Dussopt, R. Sauleau, P. Potier, and P. Pouliguen, "Wideband 400-element electronically reconfigurable transmitarray in X band," *IEEE Trans. Antennas Propag.*, vol. 61, no. 10, pp. 5017–5027, Oct. 2013.

[22] W. Pan, C. Huang, X. Ma, B. Jiang, and X. Luo, "A dual linearly polarized transmitarray element with 1-bit phase resolution in X-band," *IEEE Antennas Wireless Propag. Lett.*, vol. 14, pp. 167–170, 2015.

[23] B. Rana, I.-G. Lee, and I.-P. Hong, "Experimental characterization of 2×2 electronically reconfigurable polarization converter unit cells at X-band," *Int. J. Antennas Propag.*, vol. 2021, Jun. 2021, Art. no. 5536864.

[24] M. Wang, S. Xu, F. Yang, and M. Li, "Design and measurement of a 1-bit reconfigurable transmitarray with subwavelength H-shaped coupling slot elements," *IEEE Trans. Antennas Propag.*, vol. 67, no. 5, pp. 3500–3504, May 2019.

[25] C. Huang, W. Pan, X. Ma, and X. Luo, "1-bit reconfigurable circularly polarized transmitarray in X-band," *IEEE Antennas Wireless Propag. Lett.*, vol. 14, pp. 448–451, 2015.

[26] J. Y. Lau and S. V. Hum, "Analysis and characterization of a multipole reconfigurable transmitarray element," *IEEE Trans. Antennas Propag.*, vol. 59, no. 1, pp. 70–79, Jan. 2011.

[27] J. Y. Lau and S. V. Hum, "Reconfigurable transmitarray design approaches for beamforming applications," *IEEE Trans. Antennas Propag.*, vol. 60, no. 12, pp. 5679–5689, Dec. 2012.

[28] B. Rana, I.-G. Lee, and I.-P. Hong, "Experimental characterization of 2×2 electronically reconfigurable 1 bit unit cells for a beamforming transmitarray at X band," *J. Electromagn. Eng. Sci.*, vol. 21, no. 2, pp. 153–160, Apr. 2021.

[29] M. Frank, F. Lurz, R. Weigel, and A. Koelpin, "Electronically reconfigurable 6×6 element transmitarray at K-band based on unit cells with continuous phase range," *IEEE Antennas Wireless Propag. Lett.*, vol. 18, pp. 796–800, 2012.

[30] B. D. Nguyen and C. Pichot, "Unit-cell loaded with PIN diodes for 1-bit linearly polarized reconfigurable transmitarrays," *IEEE Antennas Wireless Propag. Lett.*, vol. 18, no. 1, pp. 98–102, Jan. 2019.

[31] L. Di Palma, A. Clemente, L. Dussopt, R. Sauleau, P. Potier, and P. Pouliguen, "Experimental characterization of a circularly polarized 1 bit unit cell for beam steerable transmitarrays at Ka-band," *IEEE Trans. Antennas Propag.*, vol. 67, no. 2, pp. 1300–1305, Feb. 2019.

[32] J. R. Reis, M. Vala, and R. F. S. Caldeirinha, "Review paper on transmitarray antennas," *IEEE Access*, vol. 7, pp. 94171–94188, 2019.

[33] M. U. Afzal and K. P. Esselle, "Steering the beam of medium-to-high gain antennas using near-field phase transformation," *IEEE Trans. Antennas. Propag.*, vol. 65, no. 4, pp. 1680–1690, Apr. 2017.

[34] M. U. Afzal and K. P. Esselle, "A low-profile printed planar phase correcting surface to improve directive radiation characteristics of electromagnetic band gap resonator antennas," *IEEE Trans. Antennas Propag.*, vol. 64, no. 1, pp. 276–280, Jan. 2016.

BISWARUP RANA received the Ph.D. degree from the Indian Institute of Engineering Science and Technology (IIEST), Shibpur, India, in 2017.

He was as a Postdoctoral Researcher with the Seoul National University of Science and Technology, South Korea. He is currently working with Kongju National University, South Korea. His research interests include analysis and design of microstrip antennas, substrate integrated waveguide antennas, phased array antennas, dielectric resonator antennas, implantable antenna, and transmitarray.

IN-GON LEE received the M.S. and Ph.D. degrees in information and communication engineering from Kongju National University, Cheonan, South Korea, in 2016 and 2020, respectively. He is currently a Postdoctoral Research Fellow with Kongju National University. His research interest includes periodic electromagnetic structures.

IC-PYO HONG (Member, IEEE) received the B.S., M.S., and Ph.D. degrees in electronics engineering from Yonsei University, Seoul, South Korea, in 1994, 1996, and 2000, respectively. From 2000 to 2003, he was with the Information and Communication Division, Samsung Electronics Company, Suwon, South Korea, where he was a Senior Engineer with CDMA Mobile Research. Since 2003, he has been with the Department of Information and Communication Engineering, Kongju National University, Cheonan, South Korea, where he is currently a Professor. In 2006 and 2012, he was a Visiting Scholar with the Texas A&M University, College Station, TX, USA, and Syracuse University, Syracuse, NY, USA, respectively. His research interests include numerical techniques in electromagnetics and periodic electromagnetic structures.

• • •